PCCP

Accepted Manuscript

ROYAL SOCIETY OF CHEMISTRY

www.rsc.org/pccp

Cite this: DOI: 10.1039/c0xx00000x

www.rsc.org/xxxxxx

ARTICLE TYPE

Theoretical investigation of the ability of borazine-melamine polymer as novel candidate for hydrogen storage applications

Hossein A. Dabbagh,*[a] Maryam Shahraki[a] and Hossein Farrokhpour*[a]

Received (in XXX, XXX) Xth XXXXXXXXX 20XX, Accepted Xth XXXXXXXXX 20XX

DOI: 10.1039/b000000x

Ab initio calculations and molecular dynamic simulation were employed to study the interaction of molecular hydrogen with the borazine-melamine polymer (BMP) in order to explore its potential for hydrogen storage applications. The calculations were performed at the long range corrected version of density functional theory using the Coulomb-attenuating method (CAM-B3LYP) and the second order Møller–Plesset perturbation theory (MP2). The results showed that the average adsorption energy per hydrogen is about -0.7 and -0.3 kcal/mol at the MP2/6-311+G(d,p) and CAMB3LYP/6-311+G(d,p) levels of theory, respectively. The adsorption energies were corrected for the basis set superposition error (BSSE) by the counterpoise method. It was found that the hydrogen storage capacity of the BMP is about 6.49 wt % which is close to the values reported for the other selected materials for the hydrogen storage in the literature. The maximum numbers of hydrogen molecules which was adsorbed by BMP building block is about ten. Molecular dynamic simulation was performed to assess the potential of BMP for hydrogen storage.

1. Itroduction

Hydrogen is essentially the only practical remedy for the growing world energy problems and is a very attractive alternative energy vector for replacing fossil fuel based economy. The future hydrogen economy offers a potential solution to satisfy the global energy requirements while reducing carbon dioxide and other greenhouse gas emissions from the atmosphere and improving energy security.[1-3] Hydrogen is everywhere, clean, efficient and environmentally friendly because, the by-product from its burning process is mainly water. Nevertheless, one of the considerable challenges of hydrogen economy is safe, efficient and effective storage of H_2 gas with the requirements of high gravimetric and volumetric density, fast kinetics, and favorable thermodynamics. The US Department of Energy (DOE) targets for commercialized hydrogen storage tanks necessitate that the gravimetric density should be 5.5 wt% and the volumetric capacity should be 40 g of hydrogen/L in 2017 for on-board hydrogen storage systems.[4]

The physical adsorption of H_2 is very weak, while its chemical adsorption in atomic form leads to the strong binding energy.[5] It should be noted that the optimal binding energy for hydrogen should be in the range between physisorption and chemisorptions in order to obtain reversibly adsorption-desorption of hydrogen at ambient pressure and temperature.[6] Recently, many experimental and theoretical researches have focused on the use of highly porous architectures such as activated carbon,[7] metal organic frameworks (MOFs),[8-14] covalent organic frameworks (COFs),[12-21] porous organic polymers,[22, 23] zeolitic imidazolate frameworks (ZIFs) [24] and boron nanostructures [25, 26] for the physisorption storage of hydrogen.

Boron–nitrogen containing systems have attracted great interest in the field of materials chemistry due to their potential applications in storage, separation, and catalysis.[27] The hydrogen storage appears to be a promising cost effective and safe method in advanced solid materials such as highly porous structure in the near future. Borazine can incorporate into the backbone of porous organic polymer as a functionalized polar building block and improves hydrogen adsorption capacity due to develop hydrogen-framework interactions.[28] Herein, El-Kaderi and co-workers have recently reported a new family of hybrid organic-inorganic nanoporous materials which called borazine-linked polymers (BLPs) for small gas storage and separation.[29-31] BLPs are the first use of borazine in the construction of highly porous polymer with halide decorated cavities which are very similar to covalent organic frameworks (COFs).[19-21] These materials are easy to fabricate, porous, light weight, and have extremely high surface area. Here in, a novel borazine-linked polymers that is called borazine-melamine polymers (BMPs) was introduced. It is expected that these materials present all of the fundamental factors required for hydrogen storage such as high surface area, pore volume, aromaticity, and light weight properties. These materials are the subject of this investigating for hydrogen storage.

Li *et al.*[32] studied the hydrogen storage capacity of alkali metals (Li, Na, or K), alkaline-earth metals (Be, Mg, or Ca), or Ti decorated borazine by using *ab initio* calculations based on the density functional theory. They showed that either Li or Ti decorated borazine can be used as a high-capacity hydrogen storage media with the capacity of 10.4 wt % and 7.2 wt %, respectively. El-Kaderi *et al.*[31] performed theoretical

investigations on H_2, CO_2, and CH_4 adsorption onto chlorinated borazine-linked polymer to understand the gas–polymer interactions and especially the interaction of gas molecules with borazine rings using density functional theory. Their investigations showed that all of the gas molecules preferably interact with the borazine ring rather than the phenyl substituent of the nitrogen atoms, which emphasizes the importance of including polarizable building blocks in adsorbent materials.

In the present study, *ab initio* calculations were utilized to evaluate the hydrogen-adsorption capacities of BMP. The interaction between hydrogen and BMP was calculated using long range corrected version of density functional theory (CAM-B3LYP) and the second order Møller–Plesset perturbation theory (MP2). All calculations were performed at 6-311+G(d,p) basis set. In addition, the average adsorption energy of H_2 molecule and the hydrogen storage capacity of BMP was performed using molecular dynamic simulation at different temperatures.

2. Computational details

For simplicity, the borazine-melamine polymer (BMP) (Fig. 1) is denoted as BMP-H. In order to facilitate the calculations, one of the building blocks of BMP-H was considered for the calculations. This monomeric unit contains three borazine bounded to one melamine ring (Fig. 1). All unsaturated bonds are terminated with hydrogen atoms.

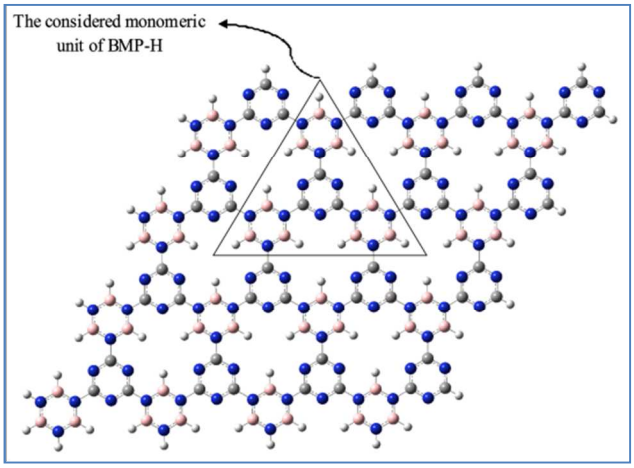

Fig.1. The proposed structure of BMP-H along with the molecular structure of its monomeric unit.

All of the calculations were performed using Gaussian 09 computational quantum chemistry package.[33] The geometry of monomeric unit was optimized at the CAM-B3LYP/6-311+G(d,p) level of theory and considered as a frozen structure in the rest of calculations. Frequency calculations were performed to confirm the minimum nature of this system (having no imaginary frequency). The CAM-B3LYP is a corrected version of B3LYP method[34] which considers long-range dispersive forces that are necessary for studying the weak interactions[35-37] such as the interaction of H_2 with nanoporous materials. To evaluate the role of the long-range dispersive forces in the interaction of H_2 molecule with BMP-H, the average adsorption energy for one H_2 molecule adsorbed on BMP-H was calculated at CAM-B3LYP/6-311+G(d,p) and Becke, 3-parameter, Lee-Yang-Parr (B3LYP)/6-311+G(d,p) methods, separately. The calculated average adsorption energy using B3LYP method is about 0.068 kcal/mol which shows that there is no tendency for adsorption of H_2 on the surface of BMP-H. Therefore, the CAM-B3LYP method was used in this work. In order to validate the levels of theories used in this work, the high level calculations were performed at the coupled cluster single double (Triple) (CCSD(T)) level of theory using 6-311+G(d,p) on the borazine with one adsorbed H_2 molecule (Fig. S1, Electronic Supplementary Information). The adsorption energy calculated at the CCSD(T) method is -0.324 kcal/mol which is very close to that obtained from MP2 (-0.349 kcal/mol) method. The calculated adsorption energy using CAM-B3LYP method is about -0.095 kcal/mol which has large deviation from the value obtained from CCSD(T) calculations. Therefore, MP2 method has been selected for all calculations in this study.

It should be mentioned that the 6-311+G(d,p) basis set were selected for the calculations because it is a relatively large size basis set and it has enough diffuse and polarization functions to describe the interactions and nearly reach the complete basis set limit. The calculations were performed using 6-311++G(df,pd) basis set on BMP-H with three hydrogen molecule and was compared with the results of 6-311+G(d,p). The calculated average adsorption energy for one hydrogen molecule was -0.174 and -0.674 kcal/mol at CAM-B3LYP and MP2 using 6-311++G(df,pd) basis set, respectively. The values calculated using 6-311+G(d,p) basis set are -0.169 and -0.631 kcal/mol at CAMP-B3LYP and MP2 levels of theory, respectively.

The adsorption energies of the BMP-H in the presence of different numbers of hydrogen molecules (one to twelve molecules) were optimized with the subsequent frequency analysis, corresponded to a minimum on a potential energy surface, at the CAM-B3LYP/6-311+G(d,p) level of theory. The optimized geometries (at the CAM-B3LYP/6-311+G(d,p) level of theory) were used to calculate the single point adsorption energies at the MP2/6-311+G(d,p) method.[38, 39] The force and energy convergence criteria was set to 3×10^{-4} and 10^{-8}, respectively for all of the calculations related to optimizations.

Adsorption energies were corrected for the basis set superposition error (BSSE) with the counterpoise method.[40] This correction is necessary since the BSSE may become important for nonbonding interactions.[41] All optimizations were followed by frequency calculations to confirm that the obtained structures represent real minima in the potential energy surface.

In addition to quantum calculations, to assess the potential of BMP-H in hydrogen gas storage, molecular dynamic simulation was performed. The simulations were performed in the canonical ensemble (N,V,T) to again estimate the Ea and compute the single component adsorption of H_2 molecule in BMP-H. The rigid structure of BMP-H was used and the universal force field (UFF) was employed in the molecular simulations. The values of the interaction potential parameters for B, C, N, H in the BMP-H and H_2 molecule is reported in Table S1 (Electronic Supplementary Information). Recently, these parameters were used by Semerci *et al.*[42] in simulation of gas storage ability of a two-dimensional coordination polymer. The Interactions between the adsorbate (H_2) and the adsorbent (BMP-H) were modeled using pair-wise interactions between hydrogen molecules and each atom in BMP-

H. Mixed-atom interactions were defined using the Lorenz-Berthelot mixing rules. The simulations were performed at 77, 150, 300 and 600 K. A simulation box (21×21×21Å) containing 245 hydrogen molecules were employed for calculations. The conventional molecular dynamic technique was used in this work to compute the average adsorption energy and hydrogen storage capacity at different temperatures. A time step equal 0.001 picoseconds were used for the simulations. A cut-off distance of 10.5 Å was used for Lennard-Jones interactions. Periodic boundary conditions were applied in the simulations. The total time for the simulation at each temperature is about 1000 picoseconds.

3. Results and discussions

3.1. Adsorption of one hydrogen molecule on different sites of BMP-H.

At first, attempt was made to find the suitable binding sites of hydrogen on the BMP-H building block by calculating the binding energy and estimating the approximate distance of H_2 molecule to the plane of the BMP-H building block. This was achieved by placing one hydrogen molecule at the top of the considered sites in two different positions (vertically and parallel) relative to the plane of BMP-H. Generally, four available sites (Fig. 2) were assigned on the BMP-H frame work. These include C atom of melamine ring (C-ring), N atom of melamine ring (N-ring), B atom of borazine ring (B-borazine) and N atom of borazine ring (N-borazine).

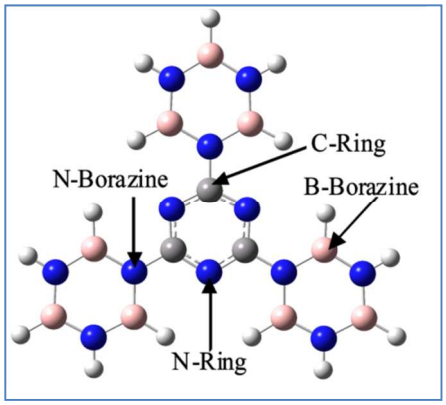

Fig. 2. The optimized structure of BMP-H at the CAM-B3LYP/6-311+G(d,p). The proposed different binding sites for H_2 adsorption have been designated. The grey, blue, pink and white colors stand for C, N, B and H atoms, respectively.

The binding energies were calculated at different intermolecular distances using the following equation:

$$Eb=E(H_2 + BMP\text{-}H) - E(BMP\text{-}H) - E(H_2) \quad (1)$$

where Eb is the BSSE corrected binding energy and $E(H_2 + BMP\text{-}H)$ is the total energies of the hydrogen adsorbed of BMP-H. E(BMP-H) and $E(H_2)$ are the counterpoise energies of the BMP-H and hydrogen molecule, respectively.

Fig. 3 shows the interaction potential energy surfaces of hydrogen molecule and the BMP-H, related to different binding sites, calculated at the MP2/6-311+G(d,p) level of theory. There is a minimum in all of the calculated surfaces indicating the ability for hydrogen molecule to bind to the BMP-H. The values of the Eb,s corresponding to the minimum energy position on the potential energy surfaces are tabulated in Table 1. It is evident that the N-Ring has the strongest interaction for the adsorption of hydrogen molecule because of its highest value of binging energy compared to the other sites when a hydrogen molecule is approaching vertically. The optimized distance between the hydrogen molecule and different sites are reported in this table. Optimum distance was measured from the lower H atom for vertical orientation. The H atom which is closer to the considered binding site was selected for parallel orientation. Based on the calculations, the optimized distance for the best site is about 3.00 Å. The optimized calculated bond length of hydrogen molecule when interacting with all active sites of BMP-H is about 0.74 Å. The calculated values of the interaction energies, reported for the different sites of BMP-H in Table 1, are in the rang of the values reported for a number of the COFs composed of B, C and O atoms by Klontzas *et al.*[43] They have shown that although the interaction of H_2 with different sites of COFs is not as strong as the interaction with the metallic doped compounds (Ti decorated borazine[32]), but some COFs with comparable surface areas with MOFs can accommodate similar amount of hydrogen gas especially at cryogenic temperatures.

3.2. Hydrogen storage capacity evaluation of BMP-H model.

First, one H_2 molecule was located at the top of B-borazine, N-borazine, N-ring and C-ring sites of the BMP-H building block at the approximate distance (3.00 Å) obtained in previous section and the geometry optimization was performed at the CAM-B3LYP/6-311+G(d,p) level of theory. It was observed that when H_2 molecule is located at the top of the B-borazine site or N-ring site, it migrates to the nearest pore site. When H_2 molecule is located at the top of the N-borazine site; it migrates to near the top of the center of borazine ring after optimization. If H_2 molecule is located at the top of the melamine ring with vertical orientation to the plane of BMP-H, the orientation is changed from vertical to parallel after optimization.

Extra calculations were performed with the initial structures when hydrogen molecule was positioned at the different bridge sites (Fig. S2, Electronic Supplementary Information). When the hydrogen molecule is located between the C and N atoms of melamine ring, the hydrogen molecule migrates to the open pore position after optimization as shown previously. When the hydrogen molecule is located between the N and B atoms of the borazine ring, it moves to the borazine ring position similar to previous case. Finally, when one hydrogen molecule was placed between the C atom of melamine ring and the N atom of borazine ring, a new position for adsorption of hydrogen molecule was obtained. Interestingly, the energy of this position is nearly equal to the borazine ring position.

Cite this: DOI: 10.1039/c0xx00000x

www.rsc.org/xxxxxx

ARTICLE TYPE

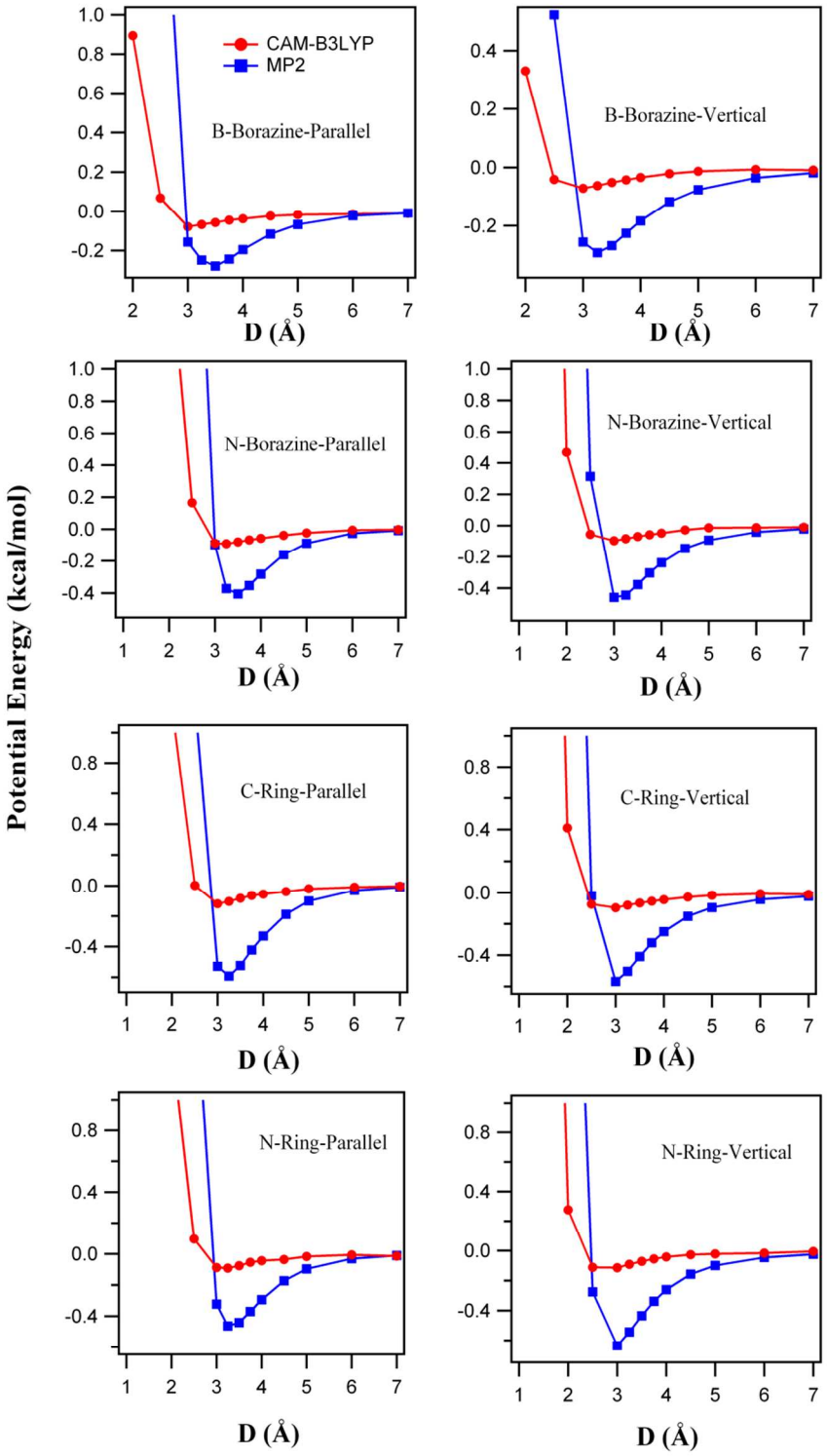

Fig. 3. The potential energies as a function of the distance between hydrogen molecule and different interaction sites for both vertical and parallel orientations to the plane, obtained from the MP2/6-311+G(d,p) and CAM-B3LYP/6-311+G(d,p) calculations.

Cite this: DOI: 10.1039/c0xx00000x

www.rsc.org/xxxxxx

ARTICLE TYPE

Table 1. Possible adsorption sites, binding energies (kcal/mol) and optimum distances [a] (Å) for adsorption of hydrogen in the BMP-H obtained from PES scans[b] using MP2/6-311+G(d,p) method.

	One H_2 adsorption			
	Vertical		Parallel	
Adsorption site	Eb[c] (kcal/mol)	H-adsorption site (Å)	Eb[c] (kcal/mol)	H-adsorption site (Å)
B-borazine	–0.294	3.2500	–0.279	3.50
N-borazine	–0.459	3.00	–0.404	3.50
C-ring	–0.568	3.00	–0.593	3.25
N-ring	–0.637	3.00	–0.464	3.25

[a] Optimum distances were measured from the lower H atom for vertical orientation and the closer H atom to the considered binding site for parallel orientation.

[b] All energy values have been BSSE corrected

[c] Binding energy.

This observation is in good agreement with the results obtained in the previous section which reveal that the BMP-H exhibits mainly three adsorption sites for H_2: (a) the top of open-pore site in BMP-H, (b) the top of borazine ring and (c) the top of melamine ring. The optimized geometries for H_2 adsorption on different adsorption sites of BMP-H are shown in Fig. 4. The BSSE corrected binding energies of these three sites have also been reported in this figure. It is evident that the optimum adsorption site of H_2 on the BMP-H system is the open-pore site with the binding energy of -0.79 kcal/mol at MP2/6-311+G(d,p) method and is the most effective adsorption site for hydrogen molecule. The H_2 molecule prefers to be adsorbed, vertically, at the top of the pore and borazine ring while it is adsorbed at the top of melamine ring parallel to the plane of molecule. Therefore, the optimized structure of BMP-H along with three H_2 molecules located at the three open pore sites was selected as the initial structure for calculating the average adsorption energy (Ea) and addition adsorption energy (E_{add}). Then, one H_2 molecule was added to this structure at different sites and the optimization was repeated for each structure. This gave the most stable geometry with four hydrogen molecule. Then, the most stable structure of BMP-H along with four H_2 molecules was selected and the fifth hydrogen molecule was added to different sites and the optimization was repeated for each structure. Similar procedure was repeated to obtain the optimized structures with more hydrogen molecules.

The average adsorption energy for H_2 molecules is defined as

$$Ea = [E(nH_2 + BMP\text{-}H) - E(BMP\text{-}H) - nE(H_2)]/n \quad (2)$$

where Ea is the BSSE corrected average adsorption energy and $E(nH_2 + BMP\text{-}H)$ is the total energies of the hydrogen molecules adsorbed on BMP-H. E(BMP-H) and $E(H_2)$ are the counterpoise energies of the BMP-H and hydrogen molecule, respectively. n is the number of adsorbed hydrogen molecules.

In order to determine the optimum hydrogen storage capacity, the BMP-H molecule was optimized with different numbers of hydrogen molecule. Fig. 5 shows the optimized structure of BMP-H with different numbers of adsorbed hydrogen molecules (n=3 to 12) without considering boundary effects. The geometry optimization showed that H_2 molecules adsorbed on BMP-H prefer to stay at the top of the pore sites rather than the borazine rings. In addition, if H_2 molecules are located at the top of the borazine rings, they migrate to one side of the borazine ring after optimizations. Also, the positions of the hydrogen molecules in the optimized structure with n numbers of hydrogen molecules do not change when it was compared with the optimized structure with n+1 numbers of hydrogen molecules. This means that the hydrogen molecules have been adsorbed on the appropriate sites. The calculated values of Ea at two different levels of theory including MP2 and CAM-B3LYP are reported in Table 2 and Table S2 of the Electronic Supplementary Information. The average adsorption energies are higher at MP2 than CAM-B3LYP level. This is related to the different consideration of the correlation electronic energy in MP2 and CAM-B3LYP methods. MP2 method is a perturbative computational method and considers more electronic correlations than DFT methods.

The distances of the adsorbed H_2 molecules from the considered sites reveal that (Table 2) by increasing the number of H_2 molecules, the H-H bond length is nearly unchanged and the H-H bond length is almost equal to that of isolated hydrogen bond length (0.7467 Å). It reveals that the interaction of hydrogen molecules with the C, N and B atoms in the BMP-H surface is physically. The values for the H_2 molecules bond length reported here are in the rang of the values in the other reports.[43]

The Mulliken atomic charge of BMP-H before and after hydrogen adsorption is reported in Table S4 of the Electronic Supplementary Information. The data indicate that BMP-H and H_2 complex is stable. For example, the partial charge of H42 and H43 is 0.002 and -0.01, respectively for the adsorbed hydrogen in the melamine ring position. The charge of all atoms of melamine ring is 0.04, -0.02, 0.15, -0.04, -0.05 and -0.003. Finally, the excess charge of -0.01 was calculated in the melamine ring. This is equal to the amount of charge transferred to the adsorbed H_2.

The BSSE correction for calculating the interaction energy of hydrogen molecules with BMP-H is necessary especially for MP2 method. For example, the calculated adsorption energy without considering the BSSE correction for BMP-H with three hydrogen molecules is about -1.381 kcal/mol while that corrected with

BSSE is -0.631 kcal/mol at MP2/6-311+G(d,p) model (Table S3, Electronic Supplementary Information).

Fig. 6 shows the variation of Ea with the number of H_2 molecules calculated at two different levels of theories which complement one another. As seen, the BMP-H with four and ten adsorbed H_2 molecules has the highest Ea among the considered structures. This means that the BMP-H with four or ten adsorbed H_2 molecules is more favorable. The hydrogen storage capacity of BMP-H was calculated 6.49 wt % based on the ten adsorbed H_2 molecules.

The addition adsorption energy (E_{add}) was calculated using equation 3 (Table 2 and S2, Electronic Supplementary Information):

$$E_{add} = E((n+1)H_2 + BMP\text{-}H) - E(nH_2 + BMP\text{-}H) - E(H_2) \quad (3)$$

where $E((n+1)H_2 + BMP\text{-}H)$, $E(nH_2 + BMP\text{-}H)$ and $E(H_2)$ are the total energies of the adsorbed hydrogen structure with n+1 and n hydrogen molecules and the hydrogen molecule, respectively. Table 2 also reports the calculated values of E_{add} for the different hydrogen molecules. Fig. 7 shows the variation of E_{add} with the increase in the number of H_2 molecules calculated at two different levels of theories. Similar trend was calculated for addition adsorption energy. Comparison of Fig. 7 with Fig. 6 shows that the variation of E_{add} with the number of hydrogen molecules is similar to the variation of Ea with the number of hydrogen molecules.

Klontzas *et al.* studied, theoretically, the hydrogen storage in three-dimensional COFs using DFT and MP2 levels of theory.[43] The calculated interaction energies for one adsorbed hydrogen molecule on different sites of COF was in the range of -0.2 to -1 and -0.06 to -0.4 kcal/mol in the case of MP2 and DFT methods, respectively when the H_2 molecule was in vertical position. A comparison of calculated adsorption energies for BMP-H (this work) with above mentioned study for COFs shows that BMP-H presents similar binding sites interaction with H_2 molecules. Therefore, it is expected that the hydrogen storage adsorption energy of BMP-H is comparable to that of COFs.

The molecular dynamic simulations were employed to estimate the value of Ea at different temperatures in order to evaluate the potential of these new materials for hydrogen adsorption at different temperatures. Typically, Fig. 8 shows snapshots of the structure of BMP-H with the adsorbed hydrogen molecules. In these snapshots, the hydrogen molecules were located at the maximum 4 Å from the surface of the BMP-H. The number of hydrogen molecules interacting with the surface of BMP-H decrease by increasing the temperature.

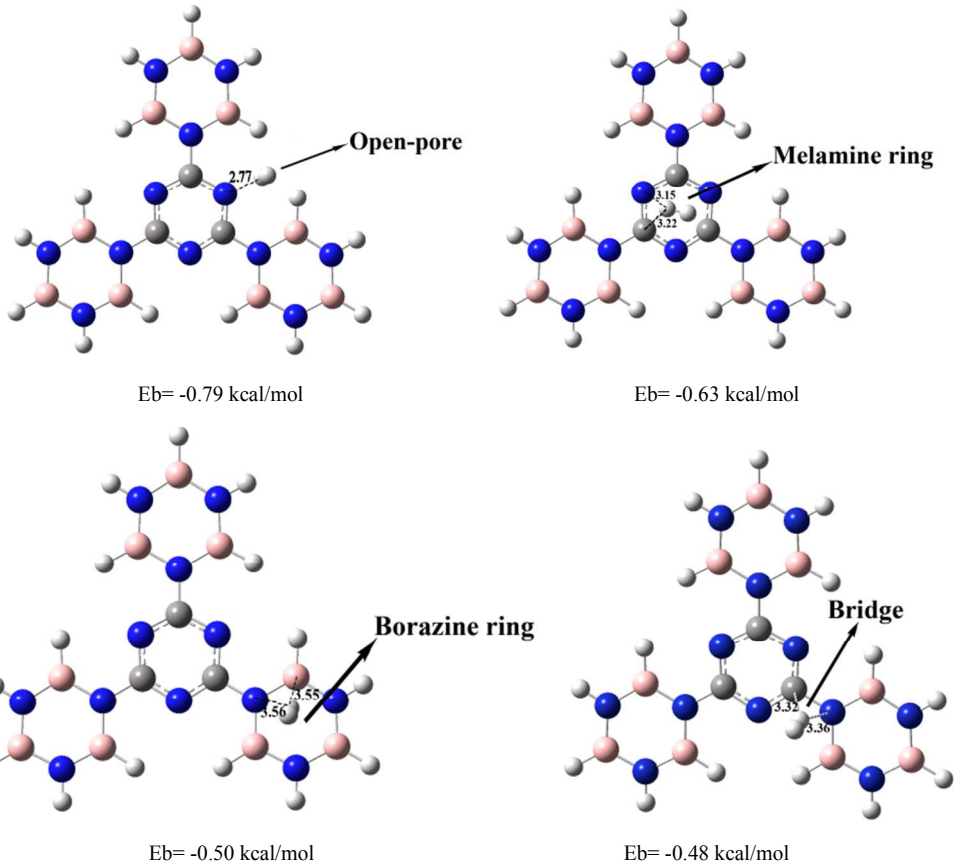

Eb= -0.79 kcal/mol | Eb= -0.63 kcal/mol

Eb= -0.50 kcal/mol | Eb= -0.48 kcal/mol

Fig. 4. The different optimized adsorption sites of H_2 molecules on BMP-H calculated at MP2/6-311+G(d,p) model. Optimum distances were measured from the lower H atom for vertical orientation and the closer H atom to the considered binding site for parallel orientation.

Cite this: DOI: 10.1039/c0xx00000x

www.rsc.org/xxxxxx

ARTICLE TYPE

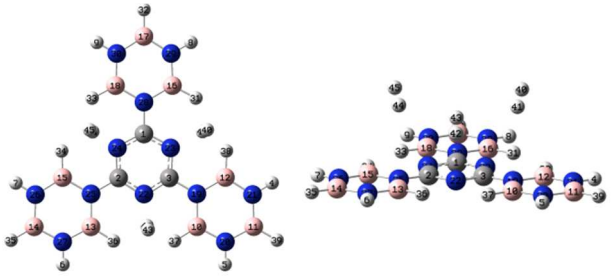

(a) $3H_2$

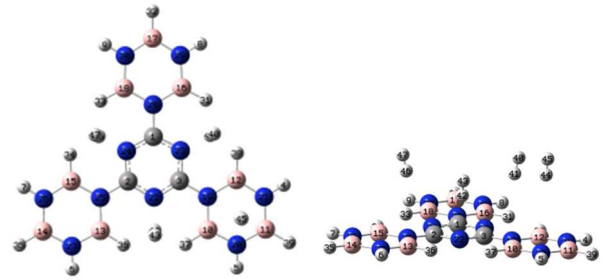

(b) $4H_2$

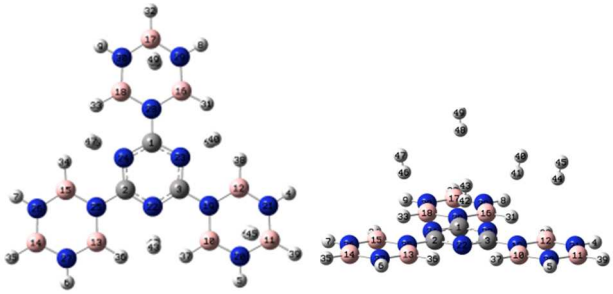

(c) $5H_2$

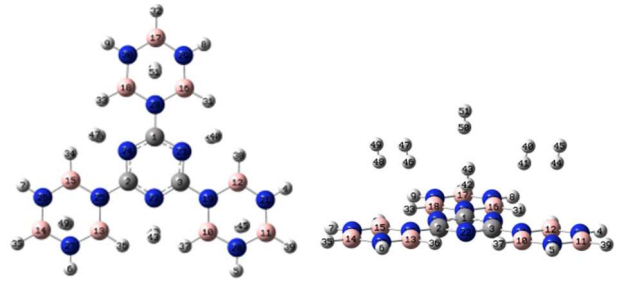

(d) $6H_2$

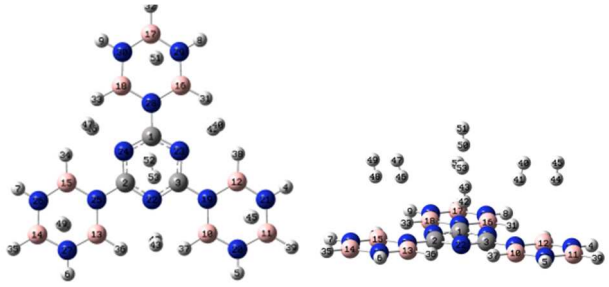

(e) $7H_2$

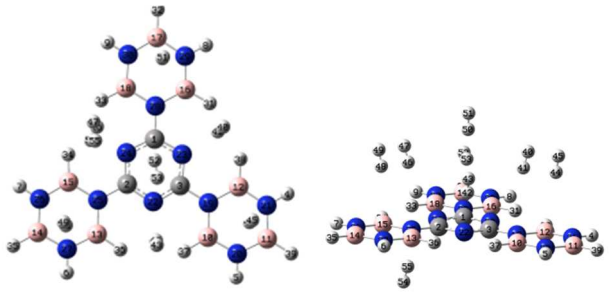

(f) $8H_2$

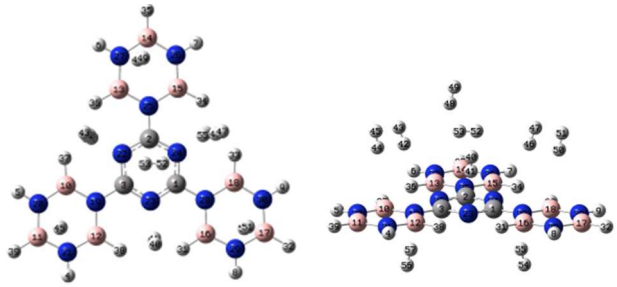

(g) $9H_2$

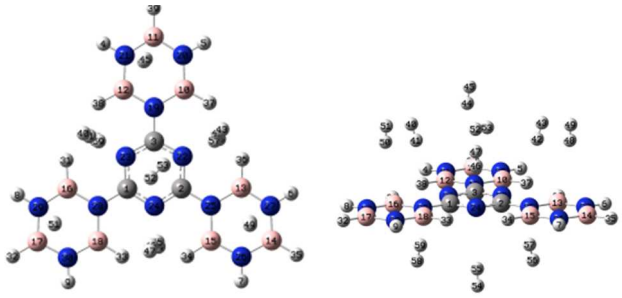

(h) $10H_2$

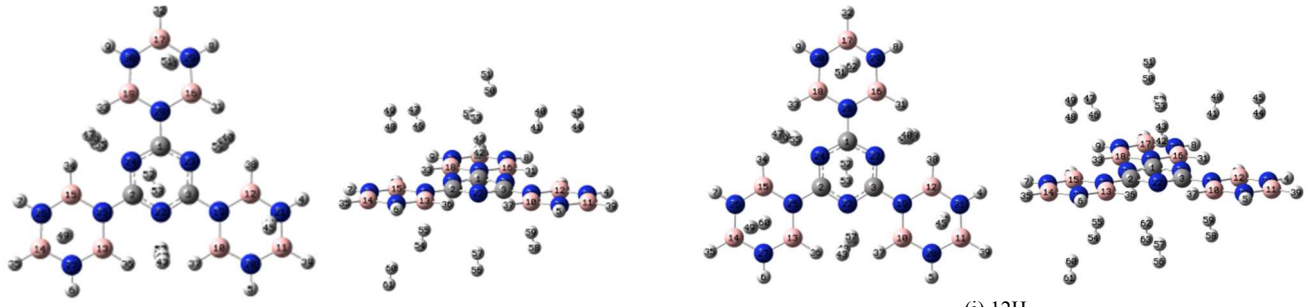

(i) $11H_2$ (j) $12H_2$

Fig. 5. The optimized capacity of BMP-H to adsorb H_2 molecules calculated at CAM-B3LYP/6-311+G(d,p) level of theory. Top and side views are given on the left and right panel, respectively. Carbon, nitrogen, boron, and hydrogen atoms are shown in grey, blue, pink and white colors, respectively.

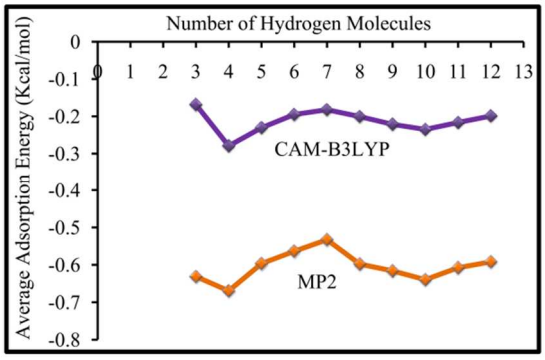

Fig. 6. Calculated average adsorption energy per H_2 as a function of the number of adsorbed hydrogen on the BMP-H.

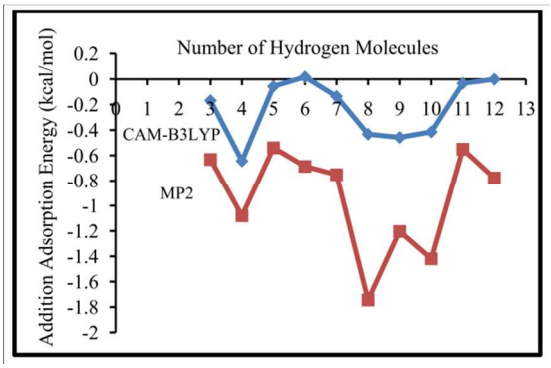

Fig. 7. Calculated addition adsorption energy as a function of the number of adsorbed hydrogen on the BMP-H.

Cite this: DOI: 10.1039/c0xx00000x

www.rsc.org/xxxxxx

ARTICLE TYPE

Table 2. Calculated bond lengths[a] (Å), average adsorption energies (kcal/mol)[b] and addition adsorption energies (kcal/mol)[b] of BMP-H adsorbed with different numbers of hydrogen molecules using MP2/6-311+G(d,p) level of theory.

		H-H (Å)	H-N (Ring)[c] (Å)	H-C[d] (Å)	H-N (Borazine)[e] (Å)	H-B[f] (Å)	Ea[g] (kcal/mol)	E_{add}[h] (kcal/mol)
$3H_2$	$1H_2$	0.7479	2.8375	-	-	3.3024	-0.631	-0.631
	$2H_2$	0.7465	3.1471	3.2291	-	-		
	$3H_2$	0.7468	-	-	3.5611	3.5555		
$4H_2$	$1H_2$	0.7478	2.8125	-	-	3.3513	-0.67	-1.08
	$2H_2$	0.7479	2.7755	-	-	3.3632		
	$3H_2$	0.7469	-	-	3.5567	3.5511		
	$4H_2$	0.7479	2.7845	-	-	3.3429		
$5H_2$	$1H_2$	0.7479	2.7855	-	-	3.349	-0.597	-0.54
	$2H_2$	0.7479	2.7907	-	-	3.3552		
	$3H_2$	0.7468	-	-	3.4702	3.4287		
	$4H_2$	0.7479	2.7826	-	-	3.3613		
	$5H_2$	0.7468	-	-	3.4777	3.439		
$6H_2$	$1H_2$	0.7478	2.8125	-	-	3.3513	-0.564	-0.686
	$2H_2$	0.7479	2.7755	-	-	3.3632		
	$3H_2$	0.7469	-	-	3.4801	3.5091		
	$4H_2$	0.7479	2.7845	-	-	3.3429		
	$5H_2$	0.7469	-	-	3.4539	3.4888		
	$6H_2$	0.7468	-	-	3.4688	3.4512		
$7H_2$	$1H_2$	0.7478	2.8354	-	-	3.3156	-0.533	-0.751
	$2H_2$	0.7478	2.8718	-	-	3.3017		
	$3H_2$	0.7470	-	-	3.3311	3.4239		
	$4H_2$	0.7477	2.9675	-	-	3.3161		
	$5H_2$	0.7472	-	-	3.1925	3.6349		
	$6H_2$	0.7467	-	-	3.2437	3.5217		
	$7H_2$	0.7465	3.2808	3.3664	-	-		
$8H_2$	$1H_2$	0.7478	2.8286	-	-	3.2996	-0.598	-1.744
	$2H_2$	0.7477	2.9496	-	-	3.309		
	$3H_2$	0.7468	-	-	3.4073	3.3806		
	$4H_2$	0.7478	2.8664	-	-	3.2855		
	$5H_2$	0.7468	-	-	3.2952	3.3544		
	$6H_2$	0.7468	-	-	3.4329	3.4099		
	$7H_2$	0.747	3.2545	3.3454	-	-		
	$8H_2$	0.7481	2.774	-	-	3.3630		
$9H_2$	$1H_2$	0.7477	2.8388	-	-	3.3328	-0.616	-1.204
	$2H_2$	0.7477	2.9096	-	-	3.3045		
	$3H_2$	0.7473	-	-	3.4762	3.3985		
	$4H_2$	0.7477	2.9216	-	-	3.2762		
	$5H_2$	0.7471	-	-	3.2854	3.394		
	$6H_2$	0.7469			3.3716	3.4050		
	$7H_2$	0.7467	3.3682	3.4206	-	-		
	$8H_2$	0.748	2.7866	-	-	3.3402		
	$9H_2$	0.748	2.7708	-	-	3.3653		
$10H_2$	$1H_2$	0.7477	2.8439	-	-	3.3168	-0.64	-1.42
	$2H_2$	0.7476	2.9505	-	-	3.3196		
	$3H_2$	0.7468	-	-	3.3451	3.3771		
	$4H_2$	0.7477	2.8849	-	-	3.3014		
	$5H_2$	0.7468	-	-	3.3816	3.3812		
	$6H_2$	0.7468	-	-	3.384	3.3909		
	$7H_2$	0.7467	3.3017	3.3895	-	-		
	$8H_2$	0.7479	2.7966	-	-	3.3564		
	$9H_2$	0.7479	2.7897	-	-	3.3652		
	$10H_2$	0.7479	2.7894	-	-	3.3551		
$11H_2$	$1H_2$	0.7478	2.8226	-	-	3.3116	-0.608	-0.551
	$2H_2$	0.7477	2.9502	-	-	3.2996		
	$3H_2$	0.7470	-	-	3.3068	3.4088		
	$4H_2$	0.7477	2.9316	-	-	3.2968		
	$5H_2$	0.7469	-	-	3.4572	3.4264		
	$6H_2$	0.7471	-	-	3.3334	3.4235		
	$7H_2$	0.7468	3.3679	3.4147	-	-		
	$8H_2$	0.748	2.7986	-	-	3.3346		
	$9H_2$	0.7479	2.7865	-	-	3.3504		

	$10H_2$	0.7478	2.7738	-	-	3.3825		
	$11H_2$	0.7467	-	-	3.5048	3.479		
$12H_2$	$1H_2$	0.7477	2.8661	-	-	3.3258	-0.592	-0.778
	$2H_2$	0.7476	2.9741	-	-	3.3268		
	$3H_2$	0.7471	-	-	3.285	3.3637		
	$4H_2$	0.7477	2.8645	-	-	3.2984		
	$5H_2$	0.747	-	-	3.4416	3.4093		
	$6H_2$	0.7468	-	-	3.4895	3.4761		
	$7H_2$	0.7469	3.2859	3.3827	-	-		
	$8H_2$	0.7479	2.784	-	-	3.3381		
	$9H_2$	0.7479	2.7943	-	-	3.3456		
	$10H_2$	0.7479	2.7990	-	-	3.3491		
	$11H_2$	0.7468	-	-	3.4871	3.465		
	$12H_2$	0.7468	-	-	3.4799	3.4558		

[a] All optimum distances were measured from the lower H atom for vertical orientation and the closer H atom to the considered binding site for parallel orientation.

[b] All energy values have been BSSE corrected

[c] Distance between H_2 and closest N-Ring

[d] Distance between H_2 and closest C-Ring

[e] Distance between H_2 and closest N-Borazine

[f] Distance between H_2 and closest B-Borazine

[g] Average adsorption energy

[h] Addition adsorption energy

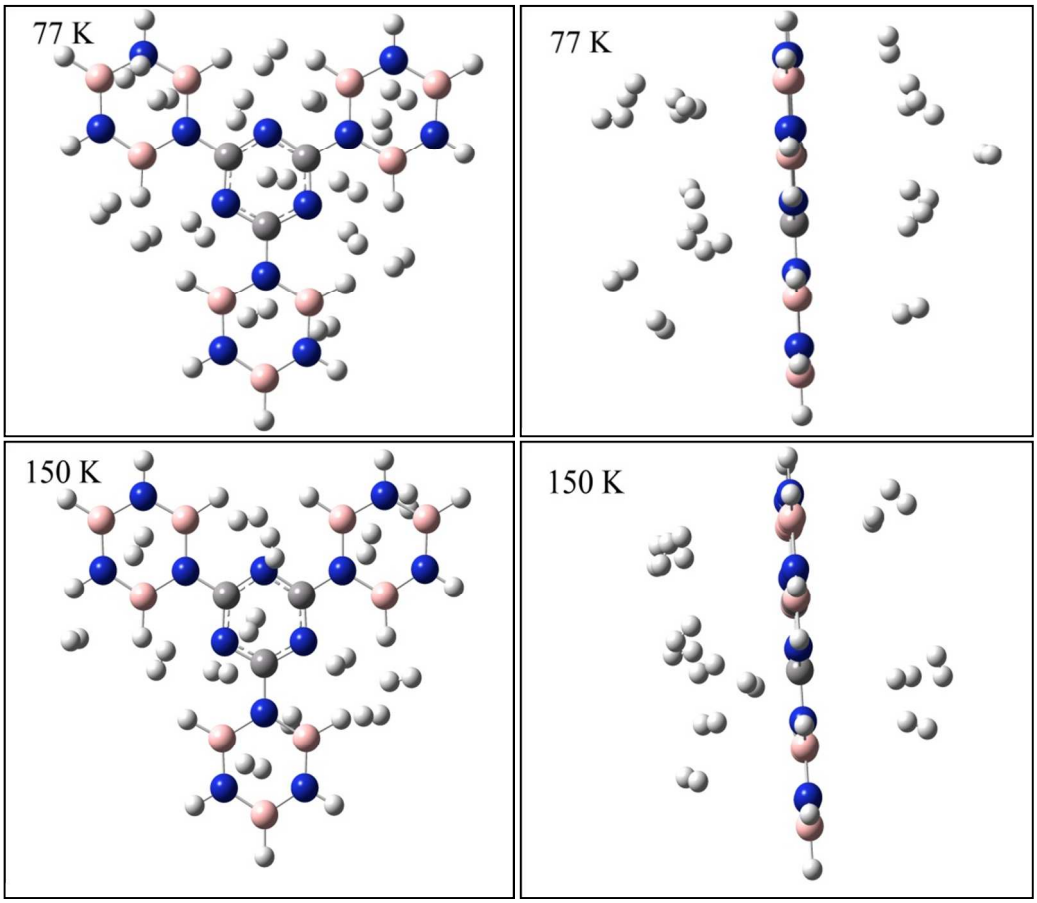

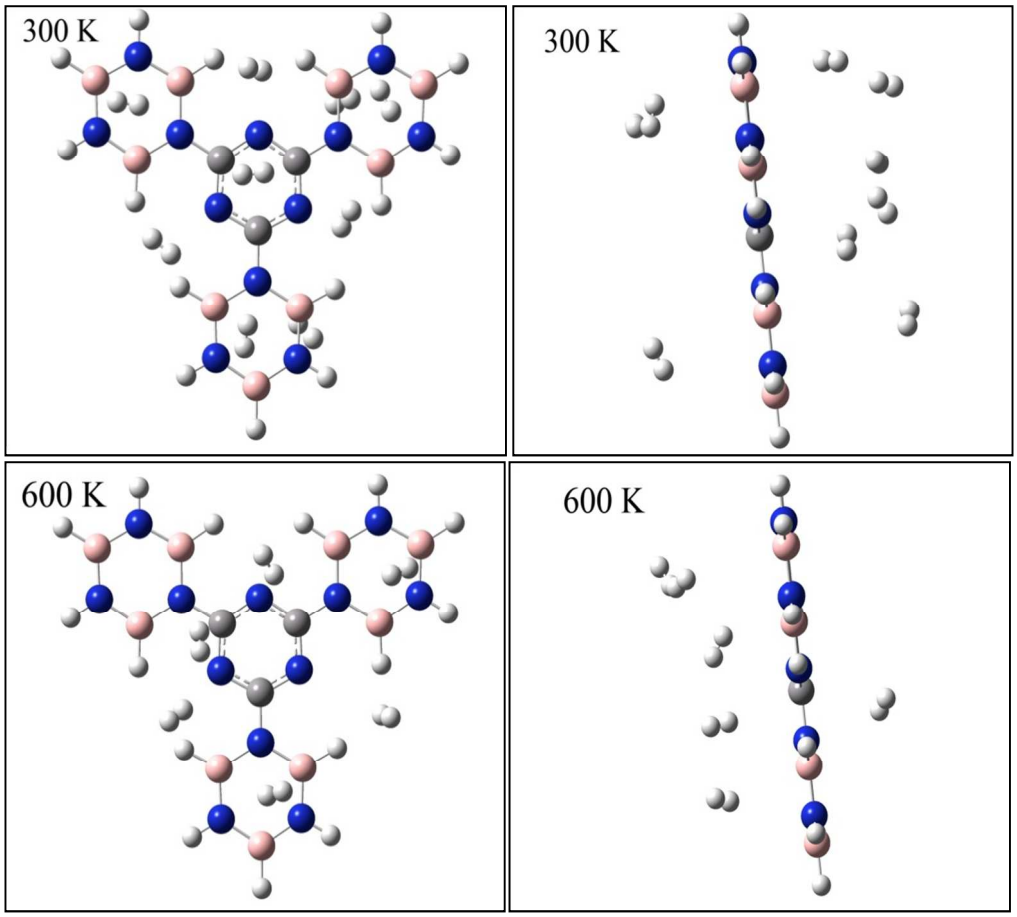

Fig. 8. Snapshots of the structure of BMP-H with adsorbed hydrogen molecules at 77, 150, 300 and 600 K. Top and side views are given on the left and right panel, respectively. Carbon, nitrogen, boron and hydrogen atoms are shown in grey, blue, pink and white colors, respectively.

To obtain the adsorption energy, a series of snapshots of the system (BMP-H+245H_2) which has been reached to thermodynamic equilibrium was selected at each temperature. These snapshots were selected from the time region where the system was reached to the thermodynamic equilibrium and the variation of the average total energy (kinetic energy + potential energy) of system was nearly independent of time. The number of snapshots selected for each temperature was about 1000 frame. The adsorption energy for each snapshot was calculated using molecular mechanic method considering UFF force field (Table S1; Electronic Supplementary Information). For this purpose, the energy of (BMP-H+245 H_2 molecules) of each snapshot was calculated using the molecular mechanic method. Then, the BMP-H molecule was removed from the snapshot and the energy of H_2 molecules was calculated. When BMP-H is removed from the snapshot, the position of H_2 molecules should not changed. In the next step, the H_2 molecules were removed and the energy of BMP-H was calculated. Finally, the binding energy for each snapshot was calculated using following equation:

$$[E(nH_2 + \text{BMP-H}) - (\text{BMP-H}) - nE(H_2)]$$

Fig. 9 shows the values of this equation (kcal/mol) was decreased by lowering the temperature.

To obtain the average adsorption energy of each snapshot, the value of binding energy was divided to the number of hydrogen molecules which are interacting with the BMP-H unit. These hydrogen molecules are mostly at the distance of 4Å from the plane of BMP-H. This procedure was repeated for all of the selected snapshots for each temperature. Then, the average of the adsorption energy of all 1000 snapshots was calculated for each temperature (Fig. 10). This figure shows decrease in the average adsorption energy at lower temperature. The values of average adsorption energy are in good agreement with those obtained using quantum calculations and confirm that this material are good candidate for hydrogen storage in the temperatures below 200 K. The hydrogen storage capacity of BMP-H is about 11.71, 10.41, 6.51 and 4.55 wt % at 77, 150, 300 and 600 K, respectively.

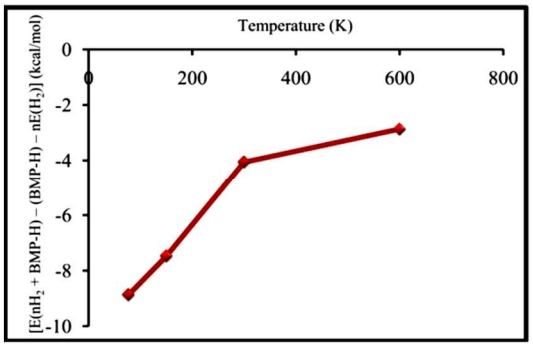

Fig. 9. The variation of the $[E(nH_2 + \text{BMP-H}) - (\text{BMP-H}) - nE(H_2)]$ as function of the temperature.

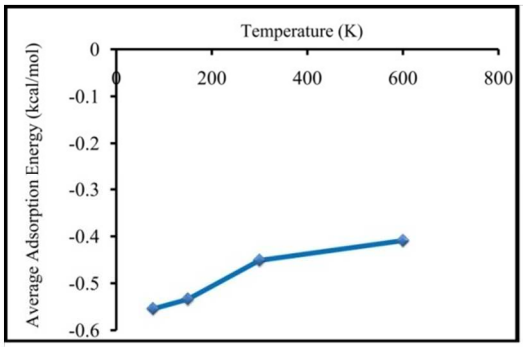

Fig. 10. Average adsorption energy of H_2 molecules as function of the temperature for BMP-H.

4. Conclusions

A comprehensive calculation was performed to study the hydrogen storage capacity of BMP-H using the density functional theory (CAM-B3LYP) and MP2 perturbation theory. The results indicated that the designated building block including melamine ring and polarizable borazine ring provides the favorable adsorption positions for hydrogen molecules. The binding strength of the hydrogen on the distinctive adsorption sites was compared with one another. It was found that, the top of open-pore site in BMP-H is the most favorable adsorption site. The CAM-B3LYP results of hydrogen adsorption on BMP building block were compared with those obtained from the MP2 calculations. The calculated average adsorption energies per hydrogen molecules are about -0.7 and -0.3 kcal/mol for MP2/6-311+G(d,p) and CAM-B3LYP/6-311+G(d,p) levels of theory, respectively which are comparable with the findings obtained from the reported materials such as COFs. The adsorption energies from MP2 are larger than that of the CAM-B3LYP level of theory and of course, are consistent with each other. The maximum number of adsorbed hydrogen molecules on the BMP-H is about ten molecules. The considered model exhibits the hydrogen storage capacity up to 6.49 wt % theoretically and attains the gravimetric 2017 DOE target. The molecular dynamic simulation was also employed to determine the hydrogen storage capacity at different temperatures. The result of this calculation showed that the BMP-H is effective compound for storing of hydrogen below 200 K. From these results, BMP-H is promising candidate for gas storage systems. It is expected that the results would assist the preparation and development of new borazine-melamine polymers for storage and separation of H_2, N_2, CO_2 and CH_4 in the future.

Acknowledgements

The authors would like to thank the Research Council of Isfahan University of Technology for cooperation.

Notes and references

[a] *Catalysis Research Laboratory, Department of Chemistry, Isfahan University of Technology, 8415483111, Isfahan, Iran*
** Tel: +98 311 391 3257; Fax: +98 311 391 2350, E-mail: dabbagh@cc.iut.ac.ir (H. A. Dabbagh), farrokhphossein@gmail.com; h-farrokh@cc.iut.ac.ir (H. Farrokhpour)*

† Electronic Supplementary Information (ESI) available: [The optimized structure of borazine with one adsorbed H_2 molecule calculated at CCSD(T) /6-311+G(d,p) level of theory (Fig. S1) and different bridge positions of H_2 molecules on BMP-H (Fig. S2) and interaction potential parameters for adsorbent and adsorbate atoms (Table S1) and calculated average adsorption energies, addition adsorption energies and BSSE values of BMP-H adsorbed with different numbers of hydrogen molecules using CAM-B3LYP/6-311+G(d,p) and MP2/6-311+G(d,p) levels of theory (Table S2 and S3) and Mulliken charge analysis of BMP-H before and after hydrogen adsorption (Table S4)]. See DOI: 10.1039/b000000x/

1. M. U. Niemann, S. S. Srinivasan, A. R. Phani, A. Kumar, D. Y. Goswami and E. K. Stefanakos, *Journal of Nanomaterials*, 2008, **2008**, 1-9.
2. R. E. Morris and P. S. Wheatley, *Angew. Chem. Int. Ed*, 2008, **47**, 4966-4981.
3. R. A.Varin, T. Czujko and Z. S. Wronski, *Nanomaterials for Solid State Hydrogen Storage*, springer, 2009.
4. Anonymous. Technical Plan-Storage. Available from, http://www1.eere.energy.gov/hydrogenandfuelcells/mypp/pdfs/storage.pdf (2012).
5. J. O. Sofo, A. S. Chaudhari and G. D. Barber, *Phys. Rev. B*, 2007, **75**, 153401.
6. R. C. Lochan and M. Head-Gordon, *Phys. Chem. Chem. Phys*, 2006, **8**, 1357-1370.
7. Z. Yang, Y. Xia and R. Mokaya, *J. Am. Chem. Soc*, 2007, **129**, 1673-1679.
8. J. L. C. Rowsell and O. M. Yaghi, *J. Am. Chem. Soc*, 2006, **128**, 1304-1315.
9. A. G. Wong-Foy, A. J. Matzger and O. M. Yaghi, *J. Am. Chem. Soc*, 2006, **128**, 3494-3495.
10. X. Zhao, B. Xiao, A. J. Fletcher, K. M. Thomas, D. Bradshaw and M. J. Rosseinsky, *Science*, 2004, **306**, 1012-1015.
11. X. Lin, J. Jia, X. Zhao, K. M. Thomas, A. J. Blake, G. S. Walker, N. R. Champness, P. Hubberstey and M. Schröder, *Angew. Chem. Int. Ed*, 2006, **45**, 7358-7364.
12. J. L. Mendoza-Cortés, S. S. Han and W. A. Goddard, *J. Phys. Chem. A*, 2011, **116**, 1621-1631.
13. M. Suri, M. Dornfeld and E. Ganz, *J. Chem. Phys*, 2009, **131**.
14. E. Ganz and M. Dornfeld, *J. Phys. Chem. C*, 2012, **116**, 3661-3666.
15. E. Tylianakis, E. Klontzas and G. E. Froudakis, *Nanoscale*, 2011, **3**, 856-869.
16. D. Kim, D. H. Jung, K.-H. Kim, H. Guk, S. S. Han, K. Choi and S.-H. Choi, *J. Phys. Chem. C*, 2011, **116**, 1479-1484.
17. Q. Yang and C. Zhong, *Langmuir*, 2009, **25**, 2302-2308.
18. G. Garberoglio, *Langmuir*, 2007, **23**, 12154-12158.
19. A. P. Côté, A. I. Benin, N. W. Ockwig, M. O'Keeffe, A. J. Matzger and O. M. Yaghi, *Science*, 2005, **310**, 1166-1170.
20. A. P. Côté, H. M. El-Kaderi, H. Furukawa, J. R. Hunt and O. M. Yaghi, *J. Am. Chem. Soc*, 2007, **129**, 12914-12915.
21. H. M. El-Kaderi, J. R. Hunt, J. L. Mendoza-Cortés, A. P. Côté, R. E. Taylor, M. O'Keeffe and O. M. Yaghi, *Science*, 2007, **316**, 268-272.
22. N. B. McKeown and P. M. Budd, *Macromol*, 2010, **43**, 5163-5176.
23. R. Dawson, A. I. Cooper and D. J. Adams, *Prog. Polym. Sci*, 2012, **37**, 530-563.
24. A. Phan, C. J. Doonan, F. J. Uribe-Romo, C. B. Knobler, M. O'Keeffe and O. M. Yaghi, *Acc. Chem. Res*, 2009, **43**, 58-67.
25. Q. Sun, Q. Wang and P. Jena, *Nano Lett*, 2005, **5**, 1273-1277.
26. G. Wu, J. Wang, X. Zhang and L. Zhu, *J. Phys. Chem. C*, 2009, **113**, 7052-7057.
27. M. Schröder, *Functional Metal-Organic Frameworks: Gas Storage, Separation and Catalysis*, Springer, 2010.
28. J. L. Belof, A. C. Stern, M. Eddaoudi and B. Space, *J. Am. Chem. Soc*, 2007, **129**, 15202-15210.
29. T. E. Reich, K. T. Jackson, S. Li, P. Jena and H. M. El-Kaderi, *J. Mater. Chem*, 2011, **21**, 10629-10632.
30. K. T. Jackson, M. G. Rabbani, T. E. Reich and H. M. El-Kaderi, *Polym. Chem*, 2011, **2**, 2775-2777.
31. T. E. Reich, S. Behera, K. T. Jackson, P. Jena and H. M. El-Kaderi, *J. Mater. Chem*, 2012, **22**, 13524-13528.
32. M. Li, J. Li, Q. Sun and Y. Jia, *J. Appl. Phys.*, 2010, **108**.

33. M. J. Frisch, G. W. Trucks, H. B. Schlegel, G. E. Scuseria, M. A. Robb, J. R. Cheeseman, G. Scalmani, V. Barone, B. Mennucci, G. A. Petersson, H. Nakatsuji, M. Caricato, X. Li, H. P. Hratchian, A. F. Izmaylov, J. Bloino, G. Zheng, J. L. Sonnenberg, M. Hada, M. Ehara, K. Toyota, R. Fukuda, J. Hasegawa, M. Ishida, T. Nakajima, Y. Honda, O. Kitao, H. Nakai, T. Vreven, J. A. Montgomery, Jr., J. E. Peralta, F. Ogliaro, M. Bearpark, J. J. Heyd, E. Brothers, K. N. Kudin, V. N. Staroverov, R. Kobayashi, J. Normand, K. Raghavachari, A. Rendell, J. C. Burant, S. S. Iyengar, J. Tomasi, M. Cossi, N. Rega, J. M. Millam, M. Klene, J. E. Knox, J. B. Cross, V. Bakken, C. Adamo, J. Jaramillo, R. Gomperts, R. E. Stratmann, O. Yazyev, A. J. Austin, R. Cammi, C. Pomelli, J. W. Ochterski, R. L. Martin, K. Morokuma, V. G. Zakrzewski, G. A. Voth, P. Salvador, J. J. Dannenberg, S. Dapprich, A. D. Daniels, O. Farkas, J. B. Foresman, J. V. Ortiz, J. Cioslowski, and D. J. Fox, Gaussian 09, Revision A.1. *Gaussian, Inc., Wallingford CT*. 2009.
34. T. Yanai, D. P. Tew and N. C. Handy, *Chem. Phys. Lett*, 2004, **393**, 51-57.
35. S. Chakrabarti and K. Ruud, *J. Phys. Chem. A*, 2009, **113**, 5485-5488.
36. N. Mohan, K. P. Vijayalakshmi, N. Koga and C. H. Suresh, *J. Comput. Chem.*, 2010, **31**, 2874-2882.
37. I. V. Rostov, R. D. Amos, R. Kobayashi, G. Scalmani and M. J. Frisch, *J. Phys. Chem. B*, 2010, **114**, 5547-5555.
38. M. Head-Gordon, J. A. Pople and M. J. Frisch, *Chem. Phys. Lett.*, 1988, **153**, 503-506.
39. M. J. Frisch, M. Head-Gordon and J. A. Pople, *Chem. Phys. Lett.*, 1990, **166**, 275-280.
40. S. F. Boys and F. Bernardi, *Mol. Phys.*, 1970, **19**, 553-566.
41. E. Klontzas, A. Mavrandonakis, Froudakis, Y. Carissan and W. Klopper, *J. Phys. Chem. C*, 2007, **111**, 13635-13640.
42. F. Semerci, O. Z. Yeşilel, M. S. Soylu, S. Keskin and O. Büyükgüngör, *Polyhedron*, 2013, **50**, 314-320.
43. E. Klontzas, E. Tylianakis and G. E. Froudakis, *J. Phys. Chem. C*, 2008, **112**, 9095-9098.